Associated Lipidomics, Metabolomics and Gut Microbiota Changes in CDAA-induced NAFLD Mice After Polyene Phosphatidylcholine Treatment

Jiayuan Zhang (zhangjiayuan3108@stu.ouc.edu.cn)
Ocean University of China
Xiaoling Zang
Ocean University of China
Jinxiao Lv
Ocean University of China
Yicong Zhang
Ocean University of China
Zhihua Lv
Ocean University of China
Mingming Yu
Ocean University of China

Research Article

Keywords: NAFLD, CDAA-induced, lipidomics, metabolomics, gut microbiota, polyene phosphatidylcholine, lysophosphatidylcholine, sphingomyelin, L-carnitine, Lactobacillus, therapeutic mechanism

Posted Date: October 25th, 2021

DOI: https://doi.org/10.21203/rs.3.rs-974725/v1

Abstract

Non-alcoholic fatty liver disease (NAFLD) is the most common chronic liver disease in most parts of the world. Currently, there is no drug approved for the treatment of NAFLD, and polyene phosphatidylcholine (PPC) is an important drug for clinical doctors to treat patients with NAFLD. Through the analysis of liver index, histopathological inspection and blood routine, it was obvious that PPC could significantly improve Choline-Deficient L-amino acid-defined (CDAA) diet induced NAFLD mice in the present work. We performed lipidomics and metabolomics analysis of 54 samples using ultraperformance liquid chromatography (UPLC) coupled to Thermo LTQ Orbitrap mass spectrometer to select differential metabolites associated with CDAA modeling and PPC treatment. A total of 19 differential metabolites including 5 polar metabolites and 14 lipids were obtained. We inferred that the protective therapeutic effect of PPC on liver was related to the supplement of phosphatidylcholine、lysophosphatidylcholine and sphingomyelin(PC, LPC, SM) and acylcarnitine metabolism. In addition, we analyzed the gut microbiota of mice before and after modeling and treatment, significant differences in the abundance of *lactobacillus* associated with NAFLD were found. This study provides more reference and data for exploring the pathogenesis of NAFLD and the therapeutic mechanism of PPC, and a methodological reference for the study of the mechanism.

1. Introduction

Nonalcoholic fatty liver disease (NAFLD) is a metabolic stress-related liver disease defined as the hepatic accumulation of lipids, mainly triglyceride, in the absence of substantial alcohol consumption (< 20 g/day) or other secondary causes[1, 2]. NAFLD has a high incidence of the disease worldwide, is one of the most common types of liver disease. An important characteristic of nonalcoholic steatosis is the accumulation of TG and TC in hepatocytes. Some patients with nonalcoholic fatty liver disease develop NASH and fibrosis, increasing the risk of cirrhosis and even hepatocellular carcinoma (HCC)[3]. Pathophysiology of NAFLD still has not been completely elucidated. Currently, the “two-hit hypothesis” proposed at the end of the 20th century is one of the most widely accepted model to explain the progression of NAFLD. The “first hit” mainly refers to the excessive accumulation of fat in liver parenchymal cells. This process has been shown to be related to insulin resistance, which can lead to a dysfunction of intracellular triglyceride synthesis and transport. The “second hit” is an oxidative stress response, which is an inflammatory reaction that occurs in liver cells on the basis of the first attack[4]. In addition, several recent studies have showed that the gut microbiota is an important factor that should be taken into account when studying NAFLD [5].

Currently, there is no approved drug for NAFLD, and polyene phosphatidylcholine (PPC) is an important drug for clinical doctors to treat patients with NAFLD[6]. The main component of PPC is extracted from soybean. The therapeutic and protective effects of PPC on liver have been reported in many studies [7, 8], However, there have been few systematic studies on its mechanism of action, and this study aims to elaborate the mechanism of PPC on non-alcoholic fatty liver from the perspective of metabolomics, lipidomics, and gut microbiota. Choline-deficient, l-amino acid-defined (CDAA) diet can interfere with fat

metabolism in the liver of mice and fat transport from liver tissues to peripheral tissues, leading to excessive fat accumulation in the liver and formation of non-alcoholic fatty liver, which is similar to the pathological state of human NAFLD patients[9, 10], Therefore, this model has been widely applied to study the therapeutic effect of drugs on NAFLD[11, 12]. In this study, we show that PPC exhibits a good therapeutic effect on CDAA diet-induced NAFLD mice using liver histopathological inspection and serum biochemical indicators, and explored possible mechanisms for the positive effects of PPC to NAFLD mice using lipidomics, metabolomics and gut microbiota analyses.

2. Materials And Methods

2.1 Animal Model.

Male C57BL/6 mice, SPF grade, purchased from Jinan Pengyue Experimental Animal Breeding Co., LTD. All healthy male mice were allowed 1 week of acclimatization before onset of the experiments. All the mice were randomly divided into two groups: a group (n = 18) was fed with choline- sufficient, l-amino acid-defined CSAA (control feed, purchased from Nantong Trophic Feed Technology Co., LTD, article number TP-0100-G), another group (n = 38) was fed with CDAA (choline deficient feed, purchased from Nantong Trophic Feed Technology Co., LTD., article number TP-0100-C). After eight weeks of feeding, two mice was chosen from each group to execute and confirm the model of fatty liver has been established successfully by liver section. The group of mice fed with CDAA was divided into two groups (CDAA/model group and PPC group) according to the weight of mice to an average. The mice fed with CSAA (negative control group) and the model group were given 10 mL/kg of normal saline every day, and the PPC group was given the same amount of PPC (15 mg/mL). The mice were weighed once a week and treated with PPC for a total of four weeks. At the end of 8 weeks, mice were fasted for 12 hours and sacrificed by. Livers and intestine were rapidly excised and flash frozen in liquid nitrogen. Blood samples were collected and centrifuged at 14000 rpm for 10 min to obtain sera samples, and all the serum and tissues samples were stored at -80 ℃ until analysis. All animal studies were conducted with the approval and following the guidelines of the Institutional Animal Care and Use Committee of Qingdao.

2.2 Histological analysis.

The liver tissue of mouse was immobilized with 4% paraformaldehyde and embedded in paraffin. The liver was sectioned and stained with hematoxylin and eosin (H&E). To observe the degree of liver fibrosis, liver sections were stained with picric acid-Sirius red solution. To observe lipid precipitation, liver tissue was frozen in tissue-Tek OCT (Tissue-Tek, Sakura Finetek, USA) and the sections were stained with oil red O reagent. All the histological procedures were performed following the standard procedures as indicated in reagent specifications. All the images were captured using an optical microscope (Nikon, ECLIPSE 80i).

2.2 Biochemical indexes analysis

Commercial kits were used to measure the contents of TG, TC, LDL-C, HDL-C, AST, ALT (Changchun Huili biotech co., ltd, Changchun, China) in mice serum according to the manufacturer's instructions.

2.3 Rat liver lipid analysis

A portion of the dissected liver tissues was ground with 9 times anhydrous ethanol. After centrifugation at 4000 g for 10 min, the supernatants were collected. Commercial kits were used to measure the contents of TG and TC (Nanjing Jiancheng Bioengineering Institute, Nanjing, China) in the liver homogenate of rats according to the manufacturer's instructions.

2.4 Lipidomics analysis

Serum samples were extracted using a method reported before[13]. A volume of 40 μL serum was mixed with 20μL internal standard mixture containing lysophosphatidylcholine (LPC) (17:0) and PC (17:0). Then 800μL chloroform/methanol (2:1, v/v) was added and shaken at room temperature for 30 minutes. Centrifuge the mixture at 14,000 rpm/min at 4°C for 10 minutes. Then the less dense lipid phase is collected and dried under vacuum at 30°C. The lipid residue was dissolved in 40 μL isopropanol/acetonitrile (1:1, v/v). Ultraperformance liquid chromatography-mass spectrometry (UPLC-MS) lipidomic profiling analyses were performed on Agilent 1290 Infinity UPLC system, equipped with Waters Acquity UPLC BEH C8 column (2.1×50 mm, 1.7 μm particle size; Waters Corporation, Milford, MA, USA), coupled to Thermo Scientific LTQ Orbitrap XL mass spectrometer. Gradient elution was employed in the chromatographic separation method using acetonitrile: water (6:4, v/v) containing 10 mM ammonium formate and 0.1% formic acid(mobile phase A) and acetonitrile: isopropanol (1:9, v/v) containing 10 mM ammonium formate and 0.1% formic acid(mobile phase B), with the following program: 0-25 min 32%-97% B, 25-29 min 97% B, 29-35 min 32% B. The flow rate was maintained at 0.25 mL/min for 35 min. Both positive and negative ionization mode data were collected, and the mass range was 200-1600 *m/z*. MS and MS/MS were collected at a resolution of 70, 000 and 17, 500, respectively. The electrospray ionization (ESI) conditions were as follows: capillary voltages and capillary Temp were set at 35 V and 300 ℃ in the positive and negative modes for the analysis. Quality control (QC) samples prepared from pooled sera of mice were used to monitor the overall quality of the lipid extraction and mass spectrometry analyses. QC samples were included in batches of analytical samples during the study. The average coefficient of variation of major lipids detected in the QC samples was < 20%. The acquired MS and MS/MS spectral data were analyzed using MSDIAL software for lipid identification according to the instructions in the software tutorial[14, 15]. The mass tolerance was set at 10 ppm.

2.5 Metabolomics analysis

A volume of 150 μL serum was mixed with 450 μL methanol and vortexed for 30 s. After centrifugation at 14000 rpm at 4 ℃ for 15 min, 500 μL of supernatant was added into a 1.5 mL centrifuge tube. The supernatant was dried under vacuum at 4 ℃ vacuum. The residue was dissolved in 100 μL acetonitrile/water (1:1, v/v) and vortexed for 30 s. The samples were centrifuged at 14,000 rpm at 4 ℃ for 15 min, and the supernatant was collected for analysis. The metabolomics analysis was performed using an Agilent 1290 Infinity UPLC system coupled to a Thermo LTQ Orbitrap mass spectrometer equipped with a heated electrospray ion source (Thermo Scientific, CA, USA). Metabolite extracts were separated on a Waters ACQUITY BEH C18 column (2.1 × 50 mm, 1.7 μm) with column temperature

maintained at 40 ℃. The mobile phase was water (A) and methanol (B), both containing 0.1% formic acid, the sample was eluted with the following program: 0-1 minutes 2% B, 1-9 minutes 2% B to 98% B, 9-12 minutes 98% B, 12-12.1 minutes 98% B to 2% B, 12.1-15 minutes 2% B. The flow rate was 250 μL/min, the sample injection volume was 8 μL. The mass spectrometer was operated in positive ionization modes. The full scan was collected at a resolution of 60,000. The data were imported to Progenesis QI software for data processing and analysis. In this experiment, compounds with p value < 0.05 and fold change value > 1.5 were considered as differential metabolites. MS/MS spectra were compared with those from online databases (HMDB: http://www.hmdb.cal and METLIN: http://metin.scrippsed) for compound identification.

2.6 Gut microbiota

With sterile scalpel, the entire intestine was taken out in a sterile state, the outer surface of the intestine was cleaned with sterile water, and the contents of the intestinal segment up to 3-4 cm of cecum were cut for intestinal microbial analysis. Microbial community genomic DNA was extracted from intestinal contents of mice using the E.Z.N.A.® soil DNA Kit (Omega Bio-tek, Norcross, GA, U.S.) according to manufacturer's instructions. The DNA extract was checked on 1% agarose gel, and DNA concentration and purity were determined with NanoDrop 2000 UV-vis spectrophotometer (Thermo Scientific, Wilmington, USA). The hypervariable region V3-V4 of the bacterial 16S rRNA gene were amplified with primer pairs 338F (5'-ACTCCTACGGGAGGCAGCAG-3') and 806R(5'-GGACTACHVGGGTWTCTAAT-3') by an ABI GeneAmp® 9700 PCR thermocycler (ABI, CA, USA). The PCR amplification of 16S rRNA gene was performed as follows: initial denaturation at 95 ℃ for 3 min, followed by 27 cycles of denaturing at 95 ℃ for 30 s, annealing at 55 ℃ for 30 s and extension at 72 ℃ for 45 s, and single extension at 72 ℃ for 10 min, and end at 4 ℃. The PCR mixtures contain 5 × TransStart FastPfu buffer 4μL, 2.5 mM dNTPs 2 μL, forward primer (5 μM) 0.8μL, reverse primer (5μM) 0.8 μL, TransStart FastPfu DNA Polymerase 0.4 μL, template DNA 10 ng, and finally ddH2O up to 20 μL. PCR reactions were performed in triplicate. The PCR product was extracted from 2% agarose gel and purified using the AxyPrep DNA Gel Extraction Kit (Axygen Biosciences, Union City, CA, USA) according to manufacturer's instructions and quantified using Quantus™ Fluorometer (Promega, USA). Purified amplicons were pooled in equimolar and paired-end sequenced on an Illumina MiSeq PE300 platform/NovaSeq PE250 platform (Illumina, San Diego, USA) according to the standard protocols by Majorbio Bio-Pharm Technology Co. Ltd. (Shanghai, China). The raw 16S rRNA gene sequencing reads were demultiplexed, quality-filtered by fastp version 0.20.0 and merged by FLASH version 1.2.7 with the following criteria. Operational taxonomic units (OTUs) with 97% similarity cutoff were clustered using UPARSE version 7.1, and chimeric sequences were identified and removed. The taxonomy of each OTU representative sequence was analyzed by RDP Classifier version 2.2 against the 16S rRNA database (eg. Silva v138) using confidence threshold of 0.7.

3. Results And Discussion

3.1 PPC has a good therapeutic effect on CDAA - modeled fatty liver in mice

As can be seen from the CDAA diet for up to two months, the weight of mice was significantly reduced compared to CSAA group, but the weight of mice was not regained by PPC administration (Figure 1A). Liver index (liver weight/body weight) is an important indicator of fatty liver. As shown in Figure 1B, we can clearly find that compared with the control group, the liver index of the CDAA group is significantly increased, and the liver index of the CSAA group is also significantly smaller than that of the CDAA group after PPC treatment. The degree of fatty liver lesions can be most intuitively seen through histological sections (Figure 2).

Accumulation of TC and TG in the liver cells is one of the most important features of NAFLD. After a long time of modeling process, the contents of TG and TC in liver homogenates in the CDAA group were significantly higher than those in the negative control group, and were significantly reduced after PPC treatment (Figure 3). Serum transaminase concentration (especially ALT and AST) is also an important indicator of liver injury. Many liver diseases lead to substantial liver damage and abnormal increase of transaminase concentration. We found that the concentration of transaminase in the serum of mice significantly increased in CDAA modeling group, indicating a relatively serious injury in the liver of mice, and significantly reduced in the PPC treatment group (Figure 4A and B). HDL and LDL levels also decreased significantly after modeling and recovered after treatment (Figure 4C and D). Choline deficiency diet may lead to defects in lipoprotein secretion[16], and PPC treatment significantly reverses these defects. Interestingly, we found the serum TG and TC levels of the model group mice were significantly decreased compared with those of the negative control (CSAA) group, and returned in some degree after PPC treatment (Figure 4E and F). This may be caused by the modeling principle of choline deficiency feeding: when choline is deficient, the content of PC decreases, and the synthesis and secretion of VLDL in the liver slows down[17], resulting in reduced rate of lipid transportation to blood and accumulation of lipids in liver cells, and finally leads to the decrease of serum lipid level. The same result was also shown in the study by Tomokatsu Miyaki et al[18], while the mechanism needs to be confirmed by further experiments.

Numerous experiments have shown that the NAFLD model caused by insufficient choline intake includes a series of processes including steatosis, fibrosis and cirrhosis, which is very similar to the development process of human NAFLD, and is suitable for human NAFLD study[19]. Histological examination is still the most accurate method for fatty liver diagnosis. Serum biochemical indicators such as (ALT) are also the most commonly used biochemical markers to assist liver function evaluation. According to the results of histological sections and biochemical indexes, after two months of CDAA diet induction, all mice in the model group developed severe fatty liver disease, and some mice also developed obvious fibrotic lesions. After one month of PPC administration (150 mg/kg), the mice in the treatment group showed significant improvement compared to the model group. These results demonstrated that this dose of PPC has a good therapeutic effect on fatty liver disease in mice. According to previous reports in the literature, PPC mainly achieves the therapeutic effect from three aspects: firstly, it provides the liver with a large amount of high-energy phospholipids, which penetrate into the liver cell membrane in the form of intact molecules, leading to increased cell membrane fluidity and liver cell regeneration[20]; secondly, it converts cholesterol into a mobile form, reducing the degeneration and necrosis of liver cells to achieve the effect

of fat removal; thirdly, it enhances the fluidity and the ability of cell membrane to absorb metabolic cholesterol of HDL, and improves the lipid metabolism of blood and liver[21]. In order to further explore its treatment mechanism, we have conducted research from the perspectives of lipidomics, metabolomics, and gut microbiota.

3.2 Effect of PPC on serum lipidome

To understand the effect of CDAA feeding on serum lipidome, lipid extracts of mice sera were analyzed using UPLC-Orbitrap mass spectrometer. Spectral data was analyzed using MSDIAL software, and eight important lipid subclasses were identified[15]. A principal component analysis (PCA) was performed for sample clustering, using the Metaboanalyst 4.0 web portal (www.metaboanalyst.ca). As shown in Figure 5, there were clear differences between CSAA and CDAA diet-fed rats serum samples, indicating considerable variation in the serum lipid composition, and PPC treated samples were well separated from CDAA group. Further analysis of the lipid abundance of each lipid class revealed that all lipid classes except phosphatidylethanolamines (PE) and ceramide (Cer) were significantly reduced after CDAA diet feeding (Figure 6A). Interestingly, the level of these lipids in the PPC treated group showed opposite result, all lipids except PE and Cer were significantly increased after PPC treatment, compared to CDAA group (Figure 6B). The alteration in TG level correspond to the results of serum biochemical analysis showing the total triglyceride content in serum of mice was reduced after long-term CDAA diet, meanwhile, the contents of PC and LPC in serum were significantly reduced. It is reported that long-term CDAA feeding leads to the decrease of PC and LPC, and the lack of PC, LPC and SM leads to the decrease in lipoprotein synthesis and secretion, resulting in decreased TG transportation from the liver to serum, accumulation of TG in the liver and a decrease of TG in the serum[22], and PPC therapy reverses this effect by supplementing PC. Table 1 and 2 show identified differential lipids (absolute value of fold change > 1.5 and p value < 0.05) between CSAA and CDAA group, and between CDAA and PPC group), respectively. Figure 6C and D show lipid species with significant differences before and after modeling and treatment. Except for PC 19:2_19:2, other lipids decreased significantly after modeling and recovered after treatment (Figure 6C and D).

Table 1
Fold changes of serum lipid species in C57BL/6 mice after CDAA diet feeding.

Lipid ID	m/z	RT(min)	Formula	Fold Change*	P Value
LPC 18:0/0:0	524.37	3.17	C26H54NO7P	-1.63	3.21E-03
LPC 18:1/0:0	522.36	1.85	C26H52NO7P	-1.66	1.70E-09
LPC 20:0/0:0	552.40	4.20	C28H58NO7P	-3.12	1.49E-09
LPC 22:0/0:0	580.44	5.31	C30H62NO7P	-2.24	1.88E-10
LPC 22:1/0:0	578.42	3.73	C30H60NO7P	-2.40	5.74E-12
LPC 22:6/0:0	568.34	1.43	C30H50NO7P	-1.76	5.97E-09
LPC 24:0/0:0	608.47	6.78	C32H66NO7P	-2.15	9.27E-10
PC 12:0_22:1	760.59	9.14	C42H82NO8P	-3.28	4.18E-05
PC 12:0_26:5	808.58	8.45	C46H82NO8P	-2.81	3.94E-04
PC 14:0_24:2	814.64	10.34	C46H88NO8P	-3.47	2.26E-13
PC 14:1_22:4	780.56	8.50	C44H78NO8P	-2.33	5.37E-08
PC 14:1_24:5	806.57	8.25	C46H80NO8P	-1.78	3.94E-08
PC 16:0_20:1	788.62	10.01	C44H86NO8P	-2.33	2.04E-10
PC 16:0_24:5	836.61	9.98	C48H86NO8P	5.36	8.29E-04
PC 17:1_17:1	758.57	8.73	C42H80NO8P	-3.29	2.77E-07
PC 17:2_17:2	754.54	8.36	C42H76NO8P	-3.12	2.00E-06
PC 18:2_18:2	782.57	8.40	C44H80NO8P	-3.60	4.26E-06
PC 19:2_19:2	810.61	9.56	C46H84NO8P	-1.96	4.74E-04
PC 20:2_18:3	808.58	8.78	C46H82NO8P	1.75	2.54E-02
PC 20:3_18:4	804.56	11.68	C46H78NO8P	-3.05	1.91E-09
PC 24:0_14:1	816.65	11.68	C46H90NO8P	-3.69	4.29E-11
PC O-35:3	756.59	7.92	C43H82NO7P	-2.23	2.12E-07
PC O-38:2	800.66	11.11	C46H90NO7P	-1.97	3.88E-07
SM 18:1;2O/14:0	675.55	7.91	C37H75N2O6P	-2.01	1.12E-06
SM 18:2;2O/16:0	701.56	8.08	C39H77N2O6P	-2.18	4.61E-09

*The CSAA Group is the reference group. “+” sign refers to abundance increase in CDAA Group, while “–” sign refers to abundance decrease in CDAA Group.

Lipid ID	m/z	RT(min)	Formula	Fold Change*	P Value
SM 18:1;2O/22:0	787.67	10.77	C45H91N2O6P	-2.52	3.60E-08
SM 18:1;2O/22:1	785.66	11.58	C45H89N2O6P	-3.72	3.66E-09
SM 18:1;2O/23:0	801.69	13.39	C46H93N2O6P	-1.63	1.15E-03
SM 18:1;2O/24:0	815.71	12.39	C47H95N2O6P	-1.62	9.68E-05

*The CSAA Group is the reference group. “+” sign refers to abundance increase in CDAA Group, while “−” sign refers to abundance decrease in CDAA Group.

Table 2
Fold changes of serum lipid species in C57BL/6 mice after PPC treatment.

Lipid ID	m/z	RT(min)	Formula	Fold Change*	P Value
LPC 18:0/0:0	524.37	3.17	C26H54NO7P	1.65	8.89E-05
LPC 19:0/0:0	538.39	3.38	C27H56NO7P	1.91	1.19E-06
LPC 20:0/0:0	552.40	4.20	C28H58NO7P	1.66	1.66E-06
LPC 20:4/0:0	544.33	1.74	C28H50NO7P	2.51	4.60E-05
LPC 22:6/0:0	568.34	1.43	C30H50NO7P	1.55	6.80E-07
PC 12:0_22:1	760.59	9.14	C44H82NO8P	1.71	2.43E-04
PC 14:1_20:2	756.56	8.50	C42H78NO8P	1.76	8.47E-04
PC 14:1_24:5	806.57	8.25	C46H78NO8P	2.49	5.88E-06
PC 16:0_22:3	812.62	10.01	C46H86NO8P	-2.51	6.82E-05
PC 16:0_24:5	836.62	9.98	C48H86NO8P	-2.18	1.82E-04
PC 17:1_17:1	758.57	8.73	C42H80NO8P	-3.96	4.88E-06
PC 17:2_17:2	754.54	8.36	C42H76NO8P	9.50	9.62E-05
PC 18:1_18:1	786.60	10.89	C44H84NO8P	-4.16	1.12E-03
PC 18:2_18:2	782.58	8.40	C44H80NO8P	1.75	1.70E-02
PC 19:2_19:2	810.61	9.56	C46H84NO8P	-1.93	3.97E-03
PC 24:0_14:1	816.65	11.68	C46H90NO8P	1.69	1.14E-04
PC O-35:1	760.62	11.95	C43H86NO7P	5.26	1.63E-04
PC O-35:3	756.59	11.10	C43H82NO7P	2.24	8.92E-05
PC O-36:1	774.64	11.44	C44H88NO7P	2.17	6.66E-04
PC O-37:1	788.65	13.09	C45H90NO7P	4.43	5.72E-05
PC O-37:5	780.58	8.33	C45H82NO7P	3.31	3.22E-04
PC O-38:1	802.67	12.32	C46H92NO7P	3.15	1.29E-05
PC O-38:2	800.66	11.63	C46H90NO7P	2.20	4.31E-08
PC O-39:3	812.66	13.46	C47H90NO7P	1.57	2.86E-05
PC O-39:4	810.62	9.71	C47H88NO7P	-2.97	7.49E-04

*The CDAA Group is the reference group. “+” sign refers to abundance increase in PPC Group, while “–” sign refers to abundance decrease in PPC Group.

Lipid ID	m/z	RT(min)	Formula	Fold Change*	P Value
PC O-40:1	830.70	13.13	C48H96NO7P	2.97	2.73E-05
SM 18:1;2O/14:0	675.55	7.91	C37H75N2O6P	1.52	1.40E-06
SM 18:1;2O/16:0	703.58	8.83	C39H79N2O6P	1.51	1.77E-10
SM 18:2;2O/16:0	701.56	8.08	C39H77N2O6P	1.56	1.96E-06
SM 18:1;2O/22:0	787.67	11.93	C45H91N2O6P	1.65	3.00E-06
SM 15:2;2O/25:0	785.66	11.17	C45H89N2O6P	1.86	1.37E-04
SM 18:1;2O/23:0	801.69	12.71	C46H93N2O6P	2.53	9.02E-06
SM 20:1;2O/21:0	701.56	11.66	C46H93N2O6P	3.29	1.09E-05
SM 22:2;2O/19:0	785.63	11.58	C46H91N2O6P	1.60	1.44E-04
SM 15:2;2O/26:6	787.67	10.77	C46H79N2O6P	2.59	1.38E-02
SM 18:1;2O/24:0	785.66	12.87	C47H95N2O6P	1.57	4.55E-06
SM 23:3;2O/20:4	801.69	13.39	C48H85N2O6P	1.77	1.26E-07

*The CDAA Group is the reference group. “+” sign refers to abundance increase in PPC Group, while “−” sign refers to abundance decrease in PPC Group.

3.3 Effect of PPC on serum metabolome

Table 3 and 4 show the differential metabolites absolute value of fold change > 1.5 and *p* value < 0.05 between CDAA and CSAA group, and between PPC and CDAA Group. It is worth noting that the levels of hexanoylcarnitine, octadecenoylcarnitine and L-carnitine were significantly decreased in the CDAA group compared to CSAA group. And after treatment with PPC, the abundances of two acylcarnitines increased significantly, while L-carnitine decreased further. Carnitine is known to be an important biological factor in fatty acid oxidation. It is essential for transporting long-chain fatty acids from the cytoplasm to the mitochondria. Acylcarnitines derived from long chain fatty acids and carnitine are transported by ester linkage to the mitochondria, where they are converted into acyl CoA on the inner mitochondrial membrane and serve as a substrate for β-oxidation[23]. L-carnitine is reported to have adjuvant therapeutic effects on fatty liver disease and insulin resistance [24–26]. PPC has been proved *in vitro* to improve the oxidative substrates of mitochondria, restore the respiratory chain activity stimulated by ADP, and improve the activity of mitochondrial cytochrome oxidase[27]. Katz et al. reported PPC can prevent oxidative phosphorylation of mitochondria and changes in mitochondrial skeleton and loss of mitochondrial cristae, and inhibit the activities of caspase-3 and caspase-9, thereby inhibiting mitochondrial apoptosis[28]. We hypothesize that PPC might alleviate the appearance of insulin resistance through the protection of mitochondria, and it might reduce the degree of fatty liver disease. According to the results, PPC might improve the absorption and utilization of L-carnitine by cells. In the PPC treatment group, L-carnitine level was further decreased but acylcarnitine levels increased, compared

to untreated group. PPC and L-carnitine might have a synergistic effect, which needs to be verified by further experiments.

Table 3
Differential metabolites between CDAA and the CSAA Group

metabolite name	m/z	RT(min)	Formula	Fold Change*	P Value
L-Phenylalanine	166.08	2.8	C9H11NO2	1.7254	0.0019
Hexanoylglycine	174.11	6.7	C8H15NO3	-1.5767	0.0477
L- Carnitine	184.09	0.8	C7H15NO3	-2.3805	0.0006
Tryptophan	227.07	4.5	C11H12N2O2	1.8593	0.0181
Hexanoylcarnitine	260.18	6.3	C13H25NO4	-4.0906	0.0069
Octadecenoylcarnitine	426.35	10.88	C25H47NO4	-1.5700	0.0033
*The CSAA Group is the reference group. “+” sign refers to abundance increase in CDAA Group, while “−” sign refers to abundance decrease in CDAA Group.					

Table 4
Differential metabolites between PPC and CDAA Group

metabolite name	m/z	RT(min)	Formula	Fold Change*	P Value
L-Phenylalanine	166.08	2.8	C9H11NO2	-1.4643	0.0307
Hexanoylglycine	174.11	6.7	C8H15NO3	1.8401	0.0002
L-Carnitine	184.09	0.8	C7H15NO3	-2.8127	0.0354
Hexanoylcarnitine	260.18	6.3	C13H25NO4	2.0028	0.0495
Glu-Ile	261.14	5.3	C11H20N2O5	-2.3478	0.0006
21-Deoxycortisol	347.22	8.8	C21H30O4	2.1645	0.0057
Octadecenoylcarnitine	426.35	10.88	C25H47NO4	2.0037	0.0001
*The CDAA Group is the reference group. “+” sign refers to abundance increase in PPC Group, while “−” sign refers to abundance decrease in PPC Group.					

3.4 Effect of PPC on gut microbiota

Abnormal changes of gut microbiota are closely related to NAFLD[5]. Therefore, in order to better explore the therapeutic mechanism of PPC on NAFLD, we further conducted gut microbiota analysis in mice. Figure 7 shows the overall difference in gut microbiota of mice in the CSAA group, CDAA group and PPC group. Studies have found that a significant feature of NAFLD patients on a high-fat diet was an increase in *Firmicutes* and a decrease in *Bacteroidetes*, this could be due to different energy residues in the faeces[29, 30]. Another reason is that the abnormal bile acid level caused by high-fat diet changes the

intestinal pH, and *Firmicutes* and *Bacteroidetes* have different adaptability to the environmental pH[31]. Different from the high-fat diet, we chose choline-deficient diet to build the NAFLD model. The weight change of mice was opposite to NAFLD patients on a high-fat diet. It is preliminarily speculated that *Firmicutes/ Bacteroidetes* are closely related to the energy in feces. Top ten genus that have significant differences among CSAA group, CDAA group and PPC group are shown in Figure 8. The most notable genus is *Lactobacillus*. Studies have shown that *Lactobacillus* is an important probiotic, which is very beneficial for maintaining health [32, 33]. Jinchi Jiang et al. isolated two *Lactobacillus* species from Chinese super-long-lived populations, and found they could regulate lipid metabolism in hypercholesterolemic rat models [34]. Experiment indicated that 20 adult patients with histologyproven NASH were randomly allocated to receive a probiotic formula containing *Lactobacillus plantarum*, *Lactobacillus delbrueckii*, *Lactobacillus acido philus*, *Lactobacillus rhamnosus* and *Bifidobacterium bifidum*, the authors found patients who had received this formula had reduced intrahepatic triglyceride content[35]. The development of NAFLD is also associated with the production of alcohol by some intestinal bacteria. A study showed that the blood and respiratory levels of ethanol in NAFLD mice were significantly higher than those in normal mice, and the activation of AMPK by *Lactobacillus rhamnoides GG* strain attenuated the accumulation of fat in the liver caused by alcohol [36]. In conclusion, studies have proved that *Lactobacillus* abundance can improve the intestinal barrier, reduce LPS levels in portal venous blood, attenuate inflammation, and inhibit fatty acid accumulation in the liver. In our study, The amount *of Lactobacillus* in CDAA group was significantly reduced compared with CSAA group, and after PPC treatment, *Lactobacillus* was significantly improved. Therefore, we speculate that PPC improves NAFLD possibly by restoring the abundance of *Lactobacilli* in NAFLD mice.

4. Conclusion

Non-alcoholic fatty liver disease (NAFLD) is a complex disease arising from both genetic and environmental factors. Our study showed that the choline deficient diet could induce mice to develop severe NAFLD and even NASH. Lipidomics, metabolomics and gut microbiota analyses combined with histopathological examination and blood routine examination had been employed to study the protective effect of PPC against CDAA-induced NAFLD mice and its possible mechanism. The content of major lipids in CDAA-induced NAFLD mice significantly changed compared with that in normal mice, and PPC treatment improved these lipid abnormalities to a certain extent, especially the lipids such as PC, LPC and SM that are associated with the synthesis of VLDL. Five metabolites were identified to have significant changes before and after modeling and treatment. The therapeutic effect of PPC on NAFLD might be related to acylcarnitine metabolism. In addition, the gut microbiota of the three groups of mice also showed significant differences. Further study is needed to elucidate the mechanism of PPC treatment on NAFLD. Our work studied the effect of PPC on NAFLD treatment *in vivo* from the perspective of lipidomics, metabolomics and gut microbiota, and provided experimental evidence for the study of PPC mechanism.

Declarations

Author contributions

Jiayuan Zhang and Mingming Yu conceived and designed the study; Jiayuan Zhang did the experiments. Jiayuan Zhang and Xiaoling Zang wrote the manuscript. All authors discussed and revised the manuscript and approved the final manuscript.

Acknowledgements

The authors thank all the staf and participants of this study for their important contributions. The data, methods used in the analysis, and materials used to conduct the research will be available to any researcher for purposes of reproducing the results or replicating the procedure from the corresponding author on reasonable request.

Conflict of interest

All authors declare that they have no conflict of interest.

Availability of data and material

The data that support the fndings of this study are available from the corresponding author on reasonable request.

Funding

This work was supported by the Fundamental Research Funds for the Central Universities [NO. 201912008] and Shandong Provincial Natural Science Foundation, China [NO. ZR2019BC025].

Ethics approval

All animal studies were conducted with the approval and following the guidelines of the Institutional Animal Care and Use Committee of Qingdao.

Consent to publication

All authors give fnal approval of the version to be published, and agree to be accountable for all aspects of the work.

References

1. Ashtari S, Pourhoseingholi MA, Zali MR. Non-alcohol fatty liver disease in Asia: Prevention and planning. World J Hepatol 2015;7:1788-1796.

2. Lazo M, Hernaez R, Eberhardt MS, Bonekamp S, Kamel I, Guallar E, Koteish A, et al. Prevalence of nonalcoholic fatty liver disease in the United States: the Third National Health and Nutrition Examination Survey, 1988-1994. Am J Epidemiol 2013;178:38-45.

3. Singh S, Allen AM, Wang Z, Prokop LJ, Murad MH, Loomba R. Fibrosis progression in nonalcoholic fatty liver vs nonalcoholic steatohepatitis: a systematic review and meta-analysis of paired-biopsy studies. Clin Gastroenterol Hepatol 2015;13:39-40.

4. Day C, James O. Steatohepatitis: a tale of two “hits”? Gastroenterology 1998;114:842-845.

5. Leung C, Rivera L, Furness JB, Angus PW. The role of the gut microbiota in NAFLD. Nat Rev Gastroenterol Hepatol 2016;13:412-425.

6. Li L, Zhang XJ, Lan Y, Xu L, Zhang XZ, Wang HH. Treatment of non-alcoholic fatty liver disease by Qianggan Capsule. Chin J Integr Med 2010;16:23-27.

7. Okiyama W, Tanaka N, Nakajima T, Tanaka E, Kiyosawa K, Gonzalez FJ, Aoyama T. Polyenephosphatidylcholine prevents alcoholic liver disease in PPARalpha-null mice through attenuation of increases in oxidative stress. J Hepatol 2009;50:1236-1246.

8. Karaman A, Demirbilek S. Protective effect of polyunsaturated phosphatidylcholine on liver damage induced by biliary obstruction in rats. Journal of Pediatric Surgery 2003;38:1341-1347.

9. Hiroko I, Kazuhiko S, Shunichi M. Morphological and functional characterization of non-alcoholic fatty liver disease induced by a methionine-choline-deficient diet in C57BL/6 mice. Int J Clin Exp Pathol 2013;6(12):2683-2696.

10. Rinella ME, Green RM. The methionine-choline deficient dietary model of steatohepatitis does not exhibit insulin resistance. J Hepatol 2004;40:47-51.

11. Cabrera D, Wree A, Povero D, Solis N, Hernandez A, Pizarro M, Moshage H, et al. Andrographolide Ameliorates Inflammation and Fibrogenesis and Attenuates Inflammasome Activation in Experimental Non-Alcoholic Steatohepatitis. Sci Rep 2017;7:3491.

12. Tolbol KS, Stierstorfer B, Rippmann JF, Veidal SS, Rigbolt KTG, Schonberger T, Gillum MP, et al. Disease Progression and Pharmacological Intervention in a Nutrient-Deficient Rat Model of Nonalcoholic Steatohepatitis. Dig Dis Sci 2019;64:1238-1256.

13. Deng P HJ, Petriello MC. Dietary inulin decreases circulating ceramides by

478 suppressing neutral sphingomyelinase expression and activity in mice. J Lipid Res 2020;61:47-51.

14. Tsugawa H, Cajka T, Kind T, Ma Y, Higgins B, Ikeda K, Kanazawa M, et al. MS-DIAL: data-independent MS/MS deconvolution for comprehensive metabolome analysis. Nat Methods 2015;12:523-526.

15. Tsugawa H, Ikeda K, Takahashi M, Satoh A, Mori Y, Uchino H, Okahashi N, et al. A lipidome atlas in MS-DIAL 4. Nat Biotechnol 2020;38:1159-1163.

16. Abdollahi-Basir MH, Shirini F, Tajik H, Ghasemzadeh MA. Zn (BDC)-(MOF): Introduction of a New Catalyst for the Synthesis Pyrimido[4,5-d]Pyrimidine Derivatives under Ultrasound Irradiation in the Absence of Solvent. Polycyclic Aromatic Compounds 2019.

17. Kulinski A, Vance DE, Vance JE. A choline-deficient diet in mice inhibits neither the CDP-choline pathway for phosphatidylcholine synthesis in hepatocytes nor apolipoprotein B secretion. J Biol Chem 2004;279:23916-23924.

18. Miyaki T, Nojiri S, Shinkai N, Kusakabe A, Matsuura K, Iio E, Takahashi S, et al. Pitavastatin inhibits hepatic steatosis and fibrosis in non-alcoholic steatohepatitis model rats. Hepatol Res 2011;41:375-385.

19. Yu Y, Cai J, She Z, Li H. Insights into the Epidemiology, Pathogenesis, and Therapeutics of Nonalcoholic Fatty Liver Diseases. Adv Sci (Weinh) 2019;6:1801585.

20. Lieber C. Pathogenesis and treatment of alcoholic liver disease: progress over the last 50 years. Rocz Akad Med Bialymst 2005;5:7□20.

21. Seitz HK, Lieber CS, Stickel F, Salaspuro M, Schlemmer HP, Horie Y. Alcoholic liver disease: from pathophysiology to therapy. Alcohol Clin Exp Res 2005;29:1276-1281.

22. Li Z, Vance DE. Phosphatidylcholine and choline homeostasis. J Lipid Res 2008;49:1187-1194.

23. Houten SM, Wanders RJA, Ranea-Robles P. Metabolic interactions between peroxisomes and mitochondria with a special focus on acylcarnitine metabolism. Biochim Biophys Acta Mol Basis Dis 2020;1866:165720.

24. Savic D, Hodson L, Neubauer S, Pavlides M. The Importance of the Fatty Acid Transporter L-Carnitine in Non-Alcoholic Fatty Liver Disease (NAFLD). Nutrients 2020;12.

25. El-Sheikh H, El-Haggar S, Elbedewy TJD, syndrome m. Comparative study to evaluate the effect of l-carnitine plus glimepiride versus glimepiride alone on insulin resistance in type 2 diabetic patients. 2019;13:167-173.

26. Xu Y, Jiang W, Chen G, Zhu W, Ding W, Ge Z, Tan Y, et al. L-carnitine treatment of insulin resistance: A systematic review and meta-analysis. 2017;26:333-338.

27. Xu Y, Leo MA, Lieber CS. DLPC attenuates alcohol-induced cytotoxicity in HepG2 cells expressing CYP2E1. Alcohol Alcohol 2005;40:172-175.

28. Katz GG, Shear NH. Signaling for ethanol-induced apoptosis and repair in vitro. Clinical Biochemistry 2001;34:219-227.

29. Jumpertz R, Le DS, Turnbaugh PJ, Trinidad C, Bogardus C, Gordon JI, Krakoff J. Energy-balance studies reveal associations between gut microbes, caloric load, and nutrient absorption in humans. Am J

Clin Nutr 2011;94:58-65.

30. Turnbaugh PJ, Ley RE, Mahowald MA, Magrini V, Mardis ER, Gordon JI. An obesity-associated gut microbiome with increased capacity for energy harvest. Nature 2006;444:1027-1031.

31. Yokota A, Fukiya S, Islam KB, Ooka T, Ogura Y, Hayashi T, Hagio M, et al. Is bile acid a determinant of the gut microbiota on a high-fat diet? Gut Microbes 2012;3:455-459.

32. Joghataei M, Shahidi F, Pouladfar G, Mortazavi SA, Ghaderi A. Probiotic potential comparison of Lactobacillus strains isolated from Iranian traditional food products and human feces with standard probiotic strains. J Sci Food Agric 2019;99:6680-6688.

33. Wang Y, Li A, Zhang L, Waqas M, Mehmood K, Iqbal M, Muyou C, et al. Probiotic potential of Lactobacillus on the intestinal microflora against Escherichia coli induced mice model through high-throughput sequencing. Microb Pathog 2019;137:103760.

34. Jiang J, Feng N, Zhang C, Liu F, Zhao J, Zhang H, Zhai Q, et al. Lactobacillus reuteri A9 and Lactobacillus mucosae A13 isolated from Chinese superlongevity people modulate lipid metabolism in a hypercholesterolemia rat model. FEMS Microbiol Lett 2019;366.

35. Vincent Wai-Sun Wong, Wong GL-H. Treatment of nonalcoholic steatohepatitis with probiotics. A proof-of-concept study. annals of hepatology 2013;12:256-262.

36. Zhang M, Wang C, Wang C, Zhao H, Zhao C, Chen Y, Wang Y, et al. Enhanced AMPK phosphorylation contributes to the beneficial effects of Lactobacillus rhamnosus GG supernatant on chronic-alcohol-induced fatty liver disease. J Nutr Biochem 2015;26:337-344.

Figures

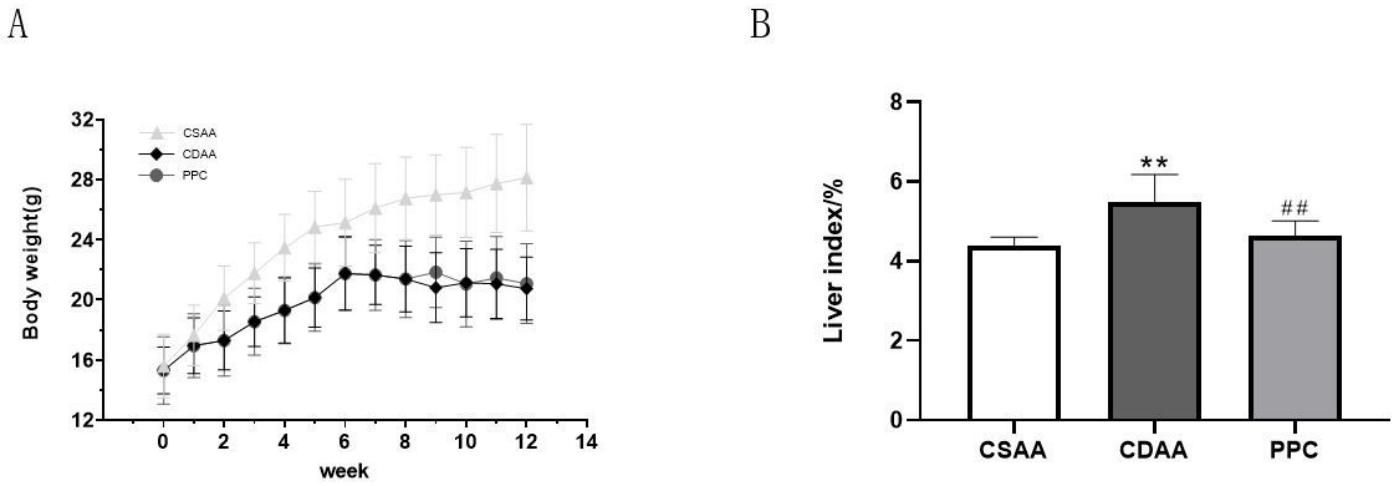

Figure 1

The body weight of mice at week 12 (A), the liver index (liver wet weight/body weight ratio) at the end of week 12 (B), *p < 0.05, ** p < 0.01 compared with negative control (CSAA diet) group; #p < 0.05, ##p < 0.01 compared with model (CDAA diet) group.

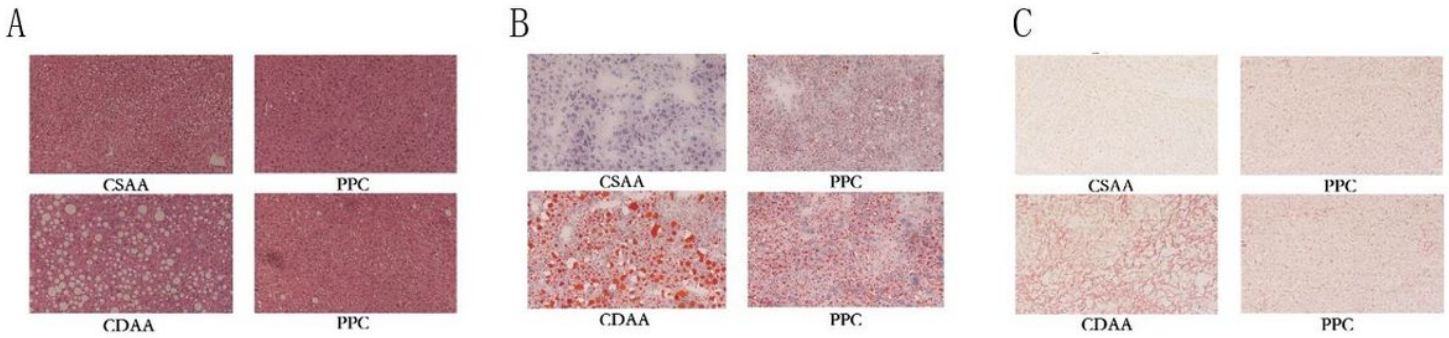

Figure 2

Section with H&E staining (A), section with oil red O staining (B) and section with Sirius red staining (C) of mouse liver tissue.

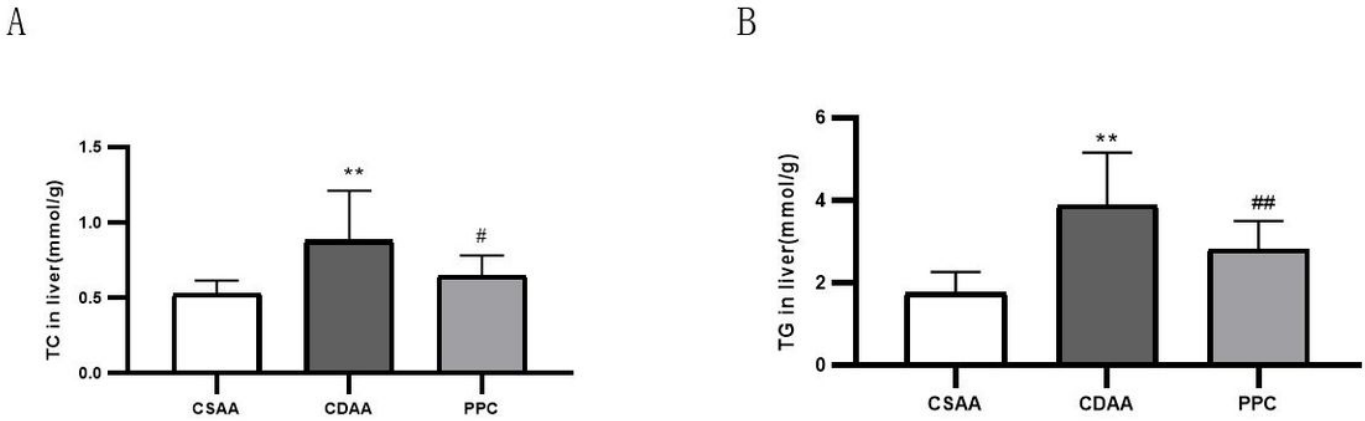

Figure 3

Biochemical measurements indicated TC (A) and TG (B) levels in liver tissue at week 12. *p < 0.05, ** p < 0.01 compared with negative control (CSAA diet) group; #p < 0.05, ##p < 0.01 compared with model (CDAA diet) group

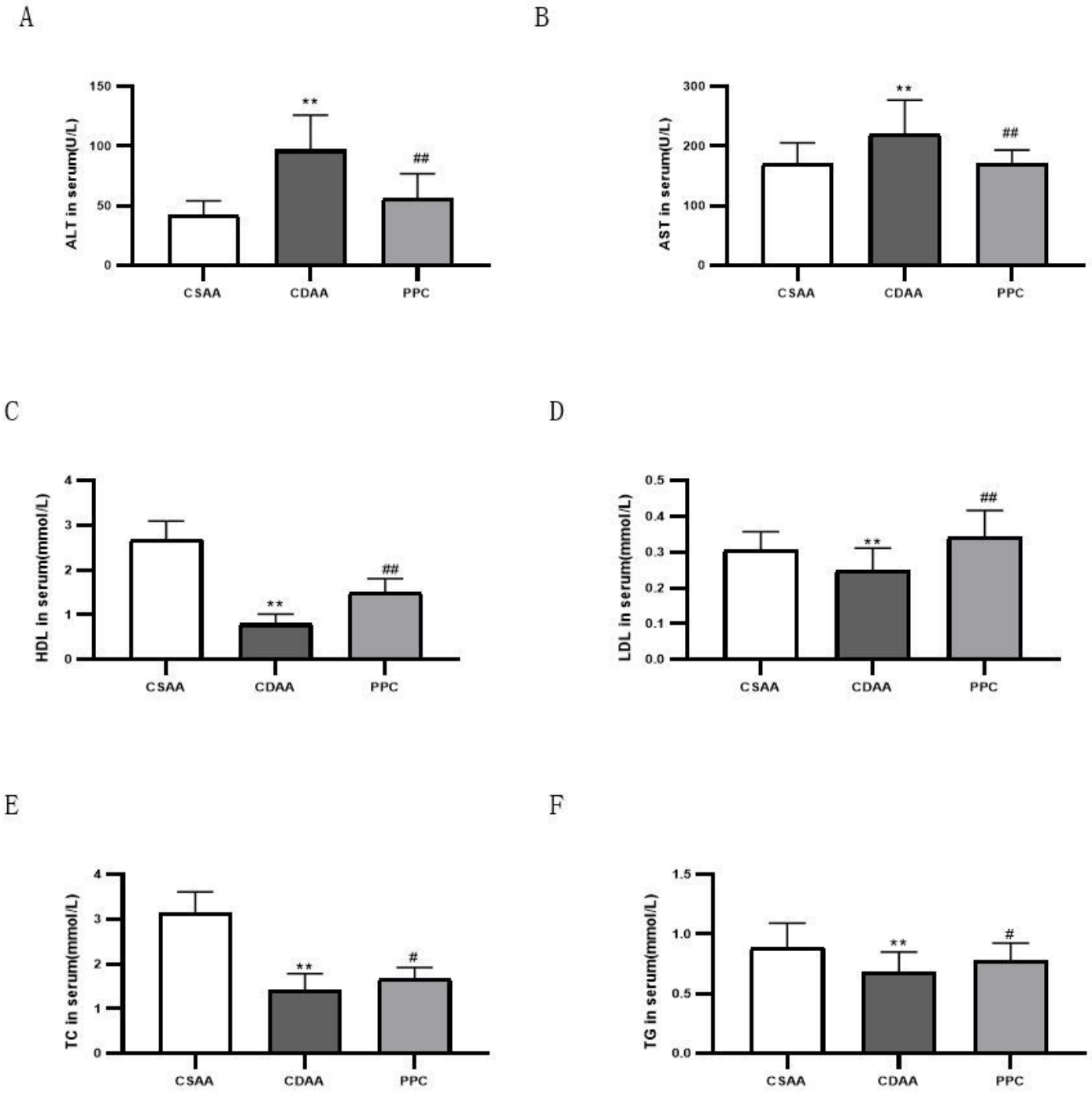

Figure 4

Serum levels of ALT (A), AST (B), HDL (C), LDL (D), TC (E) and TG (F) in CSAA, CDAA and PCC group. *p <0.05, **p <0.01 compared with negative control (CSAA diet) group; #p <0.05, ##p <0.01 compared with model (CDAA diet) group.

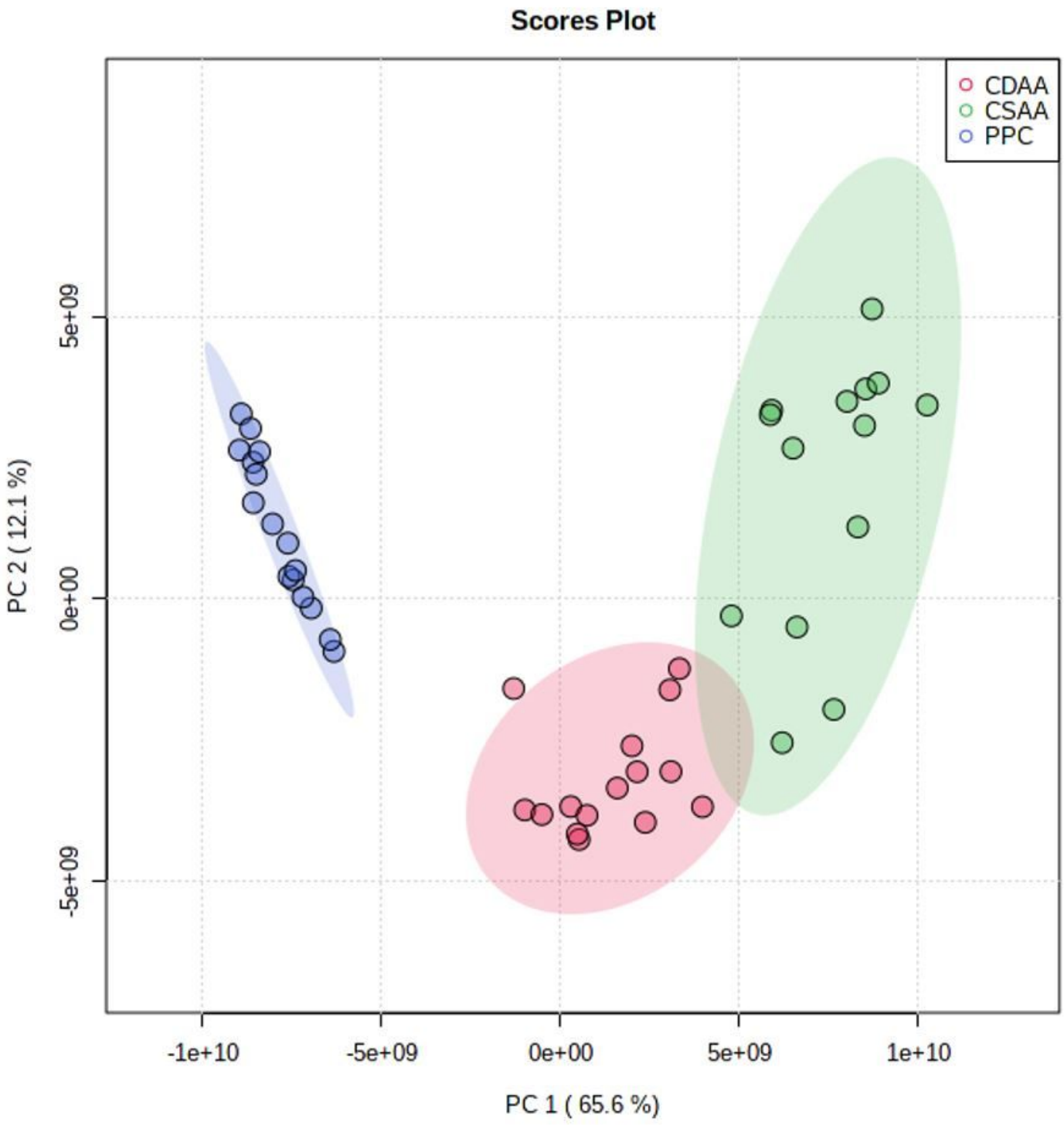

Figure 5

Principal component analysis (PCA) analysis of CSAA, CDAA and PPC group samples based on serum lipidomics data.

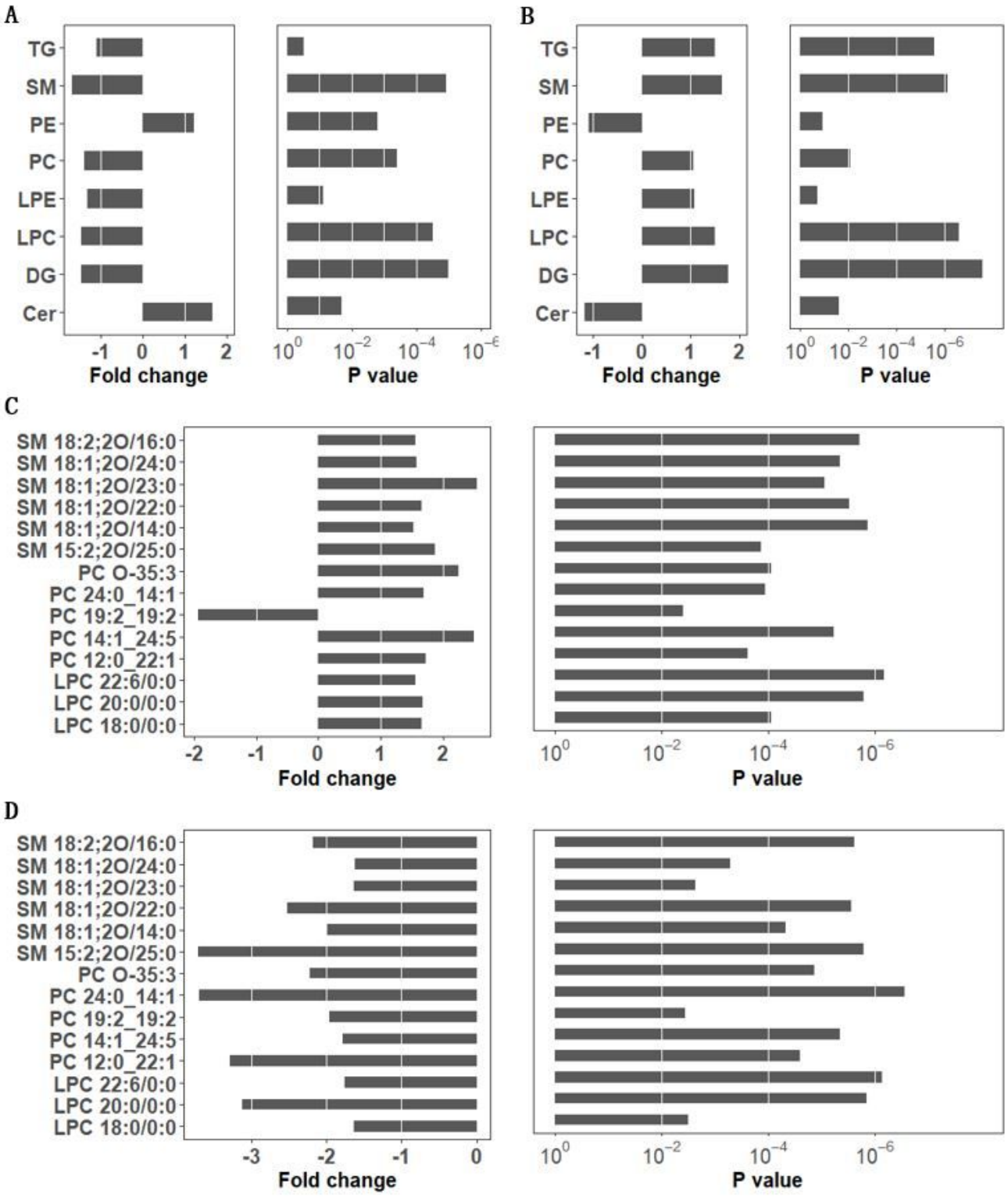

Figure 6

Fold changes of serum lipid classes before and after CDAA diet feeding (A); fold changes of serum lipid classes before and after treatment of PPC (B); fold changes of serum lipid species before and after CDAA diet feeding (C); fold changes of serum lipid species before and after treatment of PPC (D).

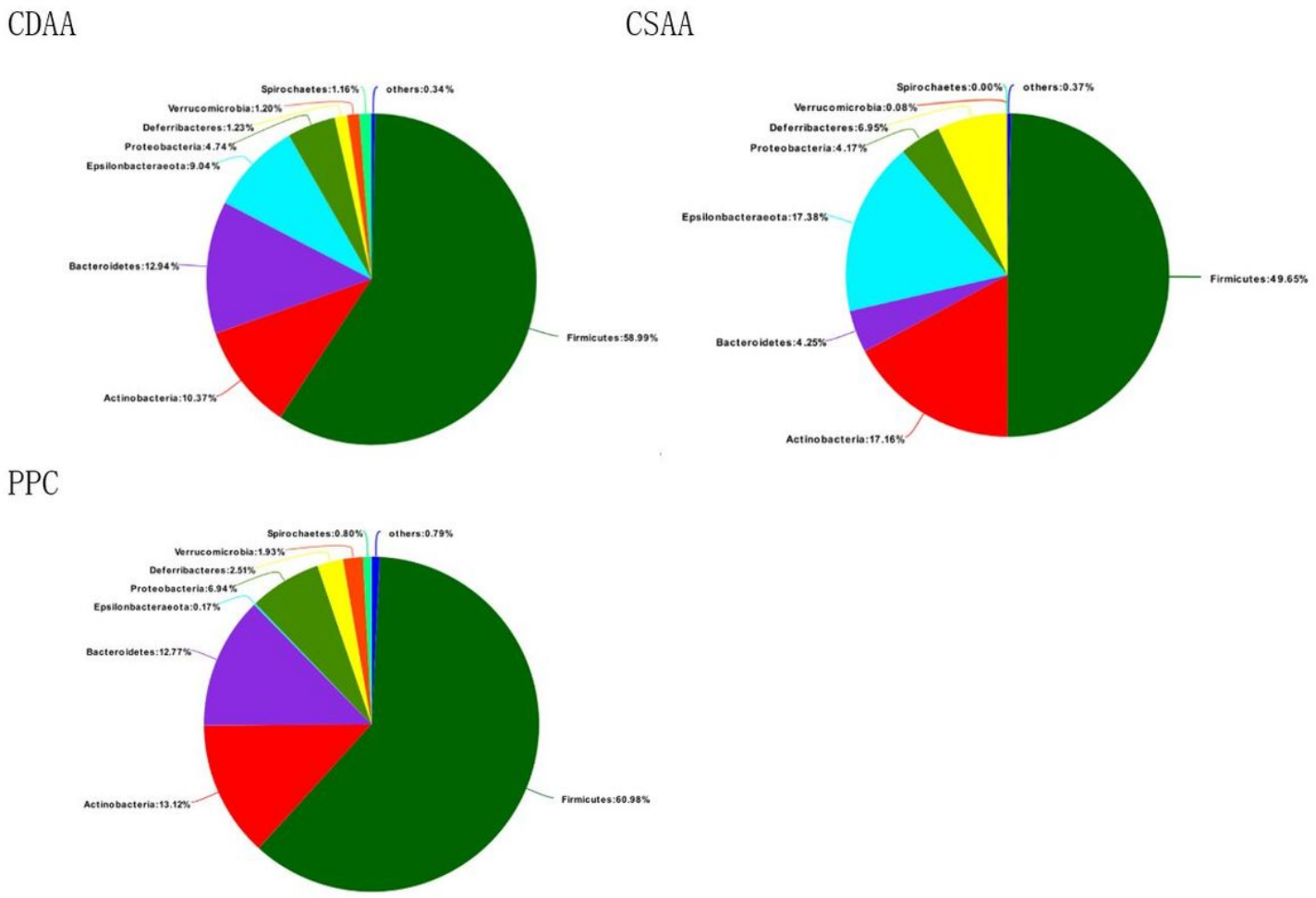

Figure 7

Average phylum distribution of gut microbiomes of CDAA group, CSAA group and PPC group.

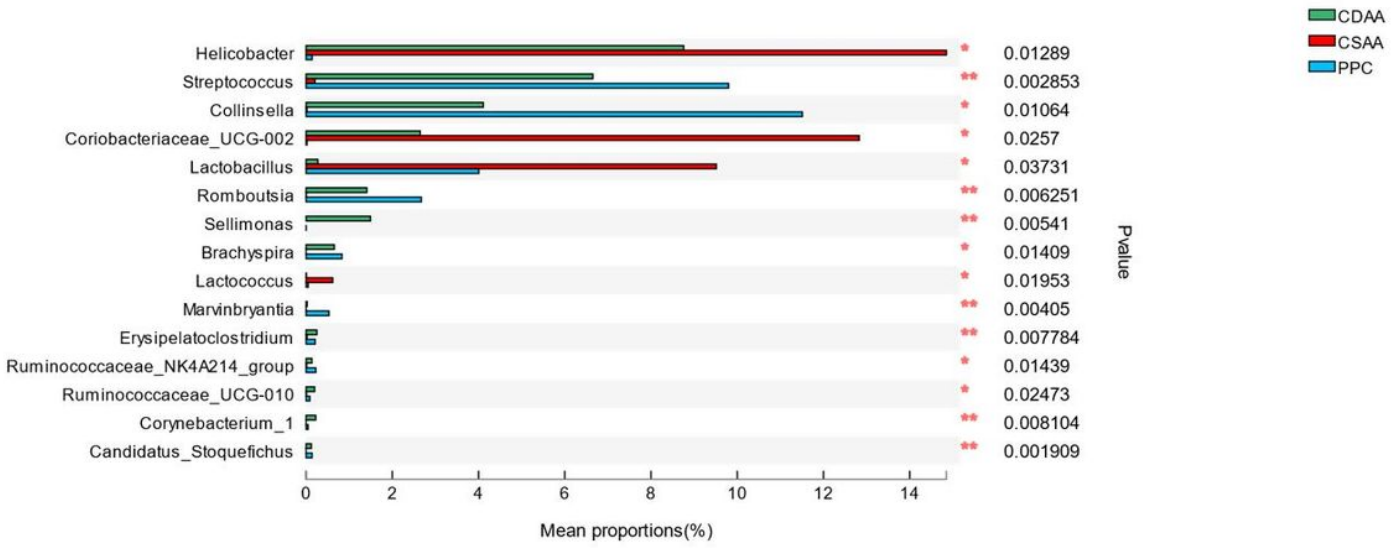

Figure 8

Top ten genus analyzed by Kruskal-Wallis test that have significant difference in relative abundance among CSAA, CDAA and PPC group.